Int. J. Electrochem. Sci., 7 **(2012)** 7675 - 7683

International Journal of ELECTROCHEMICAL SCIENCE
www.electrochemsci.org

Electrochemical Regeneration of the Cofactor NADH Employing a Carbon Nanofibers Cathode

Irshad Ali, Mark McArthur, Nathan Hordy, Sylvain Coulombe, and Sasha Omanovic[*]

Department of Chemical Engineering, McGill University; 3610 University Street, Montreal, Quebec, Canada, H3A 2B2
[*]E-mail: sasha.omanovic@mcgill.ca

Received: 5 June 2012 / *Accepted:* 16 June 2012 / *Published:* 1 August 2012

A cathode made of carbon nanofibers (CNFs) grown on a stainless steel mesh was used for the reduction of an oxidized form of the enzymatic cofactor nicotinamide adenine dinucleotide (NAD^+) to enzymatically-active 1,4-NADH, *i.e.* for the electrochemical regeneration of 1,4-NADH. The CNF cathode was shown to enable fast electrochemical NAD^+ reduction kinetics and high NAD^+ conversion relative to the glassy carbon and stainless steel mesh cathodes alone. The CNF cathode was also found to be highly selective, yielding a 99.3 ± 0.6 % pure 1,4-NADH product. As such, the CNF cathode is a good candidate for the electrochemical regeneration of 1,4-NADH in biochemical reactors and biosensors.

Keywords: Electrochemical NADH regeneration; NAD^+ reduction kinetics; Carbon nanofibers; Stainless steel mesh

1. INTRODUCTION

Co-enzyme nicotinamide adenine dinucleotide NAD(H) participates in a large number of biochemical processes, in which it acts as a hydrogen and electron carrier [1-4]. Hence, NAD(H) is found in two redox forms: oxidized NAD^+ and reduced NADH (the only enzymatically active isomer of the latter is 1,4-NADH). In industry, 1,4-NADH is of importance in enzymatic biocatalysis especially in the field of chiral compound preparation [5]. It is also used in the production of high value-added compounds (e.g. expensive drugs), and for the development of biosensors and bio-fuel cells [6-14]. However, due to its very high cost and the need to be added in a biochemical reactor in stoichiometric quantities, the current use of 1,4-NADH is very limited. A solution to this problem would be to develop *in-situ* 1,4-NADH regeneration methods. Electrochemical methods are of particular interest due to their potential low cost, simplicity and ease of product isolation.

The electrochemical regeneration of 1,4-NADH from NAD^+ is a two-step process (Fig. 1) In Step 1, NAD^+ is reduced to give a NAD-radical, which is further reduced and protonated in Step 2a to give NADH. Step 2a is considered to be slow due to the slow protonation of the NAD-radical [15-23]. This, in turns, can result in the very fast dimerization of two neighboring NAD-radicals to produce enzymatically inactive dimer, NAD_2 (Step 2b).

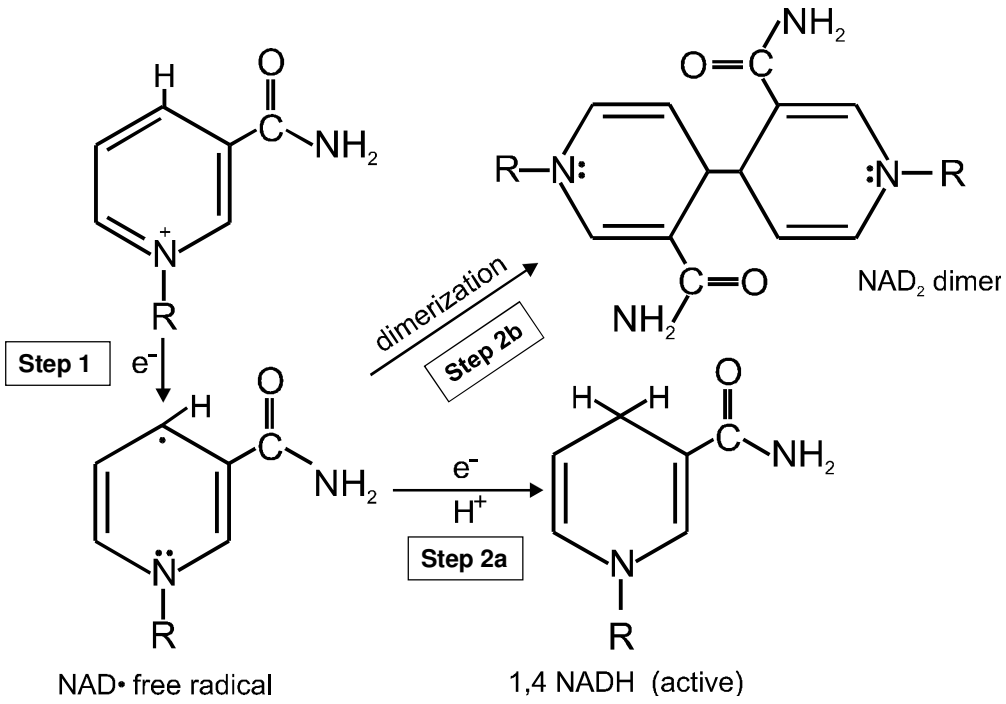

Figure 1. Reduction of NAD^+ to NAD_2 and enzymatically-active 1,4-NADH. R= adenosine diphosphoribose.

Literature reports that on bare (unmodified) electrodes, the kinetics of Step 2b is indeed significantly faster than that of Step 2a, and thus the major product of NAD^+ reduction on these electrodes is NAD_2. Consequently, the yield of enzymatically active 1,4-NADH regenerated on non-modified electrodes ranges from below 1% on a reticulated vitreous carbon [24] to 76% on Hg [22, 25-29]. However, we have demonstrated that by the modification of the electrode surface, the yield can significantly increase, reaching a 100% regeneration recovery [30]. The other interesting finding of our group was that, if the NADH regeneration is performed using a bare (non-modified) glassy carbon electrode polarized at high cathodic potentials, a 100% regeneration recovery can also be obtained [31]. The glassy carbon electrode represents a good candidate material for the regeneration of 1,4-NADH in industrial bioreactors; however, due to its low (two-dimensional) surface area, the corresponding NAD^+ conversion rate is rather slow. Obviously, one can increase the NAD^+ conversion on a glassy carbon electrode by employing a multiple electrode setup, but this would result in an increase in the electrochemical reactor volume. A solution to this problem would be to use a carbon-based surface of a very high roughness, *i.e.* very large surface-to-volume ratio. We hypothesized that

carbon nanofibers (CNFs) would fulfill this requirement, given that (i) this is a carbon-based material like glassy carbon, (ii) CNFs have a very large surface-to-volume ratio, and (iii) is a nano-sized material, thus offering an intrinsically large electro-active surface (i.e. electrochemical activity).

In this manuscript we report, for the first time, the use of CNFs deposited on a stainless steel mesh as a cathode in a batch electrochemical reactor for the regeneration of enzymatically active 1,4-NADH. CNFs were produced using a synthesis method developed in our plasma laboratory [32]. We demonstrate in this work that the NAD^+ conversion rate is increased significantly on the CNF cathode relative to the glassy carbon cathode. We also demonstrate that a 100% 1,4-NADH recovery from NAD^+ can be obtained when using the CNF cathode, thus making them suitable for large-scale applications in bioreactors.

2. EXPERIMENTAL

2.1. CNF synthesis

A stainless steel 316, 400 series mesh (25 μm grid bar, 2.5 cm × 2.5 cm sample size; cleaned ultrasonically in acetone) was used as the CNF formation/growth catalyst and support material. The support was placed within a tubular chemical vapor deposition furnace (55 mm-inner diameter quartz furnace tube), under argon (592 ± 5 cm^3 min^{-1}), and heated to 700 ^oC. Acetylene was then injected into the furnace for 4 min at a constant flow rate of 100 ± 5 cm^3 min^{-1}. This was followed by an isothermal CNF growth period of 30 min at 700 ^oC under Ar. The system was then cooled to room temperature (22 ^oC). This method of growth is based on the work by Baddour et al. [32], in which carbon nanotubes and CNFs were grown directly from stainless steel sheets. However, in the current work no pretreatment steps (acid etching) were required. Visual characterization of the CNFs was conducted using field emission scanning electron microscopy and transmission electron microscopy. The purity of the samples was tested using a thermal gravimetric analysis (TGA) in air. A temperature range of 25 to 700 ^oC was covered at a constant heating rate of 20 ^oC min^{-1}.

2.2. Electrochemical regeneration of 1,4-NADH

Electrochemical regeneration of enzymatically active 1,4-NADH from a 1 mM NAD^+ solution in 0.1 M phosphate buffer (pH = 5.8), was performed at 22 ^oC in a three-electrode, two compartment batch electrochemical reactor (cell). NAD^+ solutions were prepared by dissolving a proper amount of β-NAD^+ (sodium salt, purity 98%) in phosphate buffer. Aqueous solutions were prepared using deionized water (resistivity 18.2 MΩ cm). The stainless steel mesh (2.5 cm × 2.5 cm) covered on both sides with CNFs served as a working electrode. The total geometric area of this electrode was 12.5 cm^2. Two carbon rod counter electrodes were placed opposite of the two sides of the working electrode. In order to maintain an oxygen-free electrolyte, argon (99.998% pure) was purged through the electrolyte prior to, and during electrochemical measurements. The Ar purge also ensured convective mass transport of electroactive species to/from the electrode surface. The electrochemical

reactor was connected to a potentiostat, which was used to apply a constant potential to the working electrode. The progress of the NAD^+ reduction reaction was monitored by UV/Vis spectrophotometry.

To determine the enzymatic activity of the regenerated 1,4-NADH, activity tests were made according to the regular Sigma Quality Control Test Procedure (EC 1.8.1.4) using lipoamide dehydrogenase (5.3 U/mg) as an enzyme and DL-6,8-thioctic acid amide as a substrate[15, 33].

3. RESULTS AND DISCUSSION

3.1. Carbon nanofibers characterization

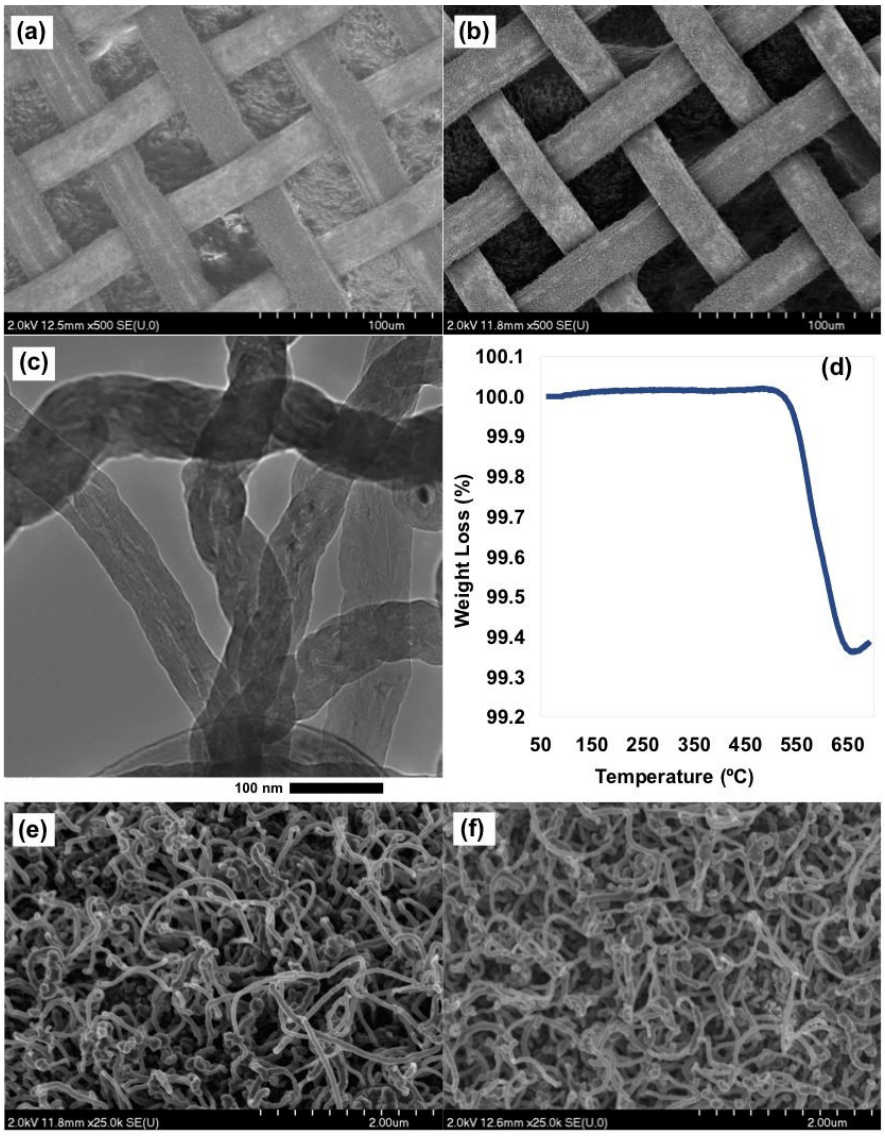

Figure 2. SEM micrographs of carbon nanofibers (*a* and *e*) before measurement, (*b* and *f*) after measurement, (*c*) TEM image and (*d*) TGA curve.

Fig. 2 shows electron micrographs of CNFs grown on the stainless steel mesh support at various magnifications. These CNFs consist of a tube-like structure, approximately 2 μm in length and 40-100 nm in diameter. Fig. 2(c) displays a transmission electron micrograph of several CNFs. It was observed that the CNFs consist of many graphene layers, some of which are parallel to the fiber axis, while others are extremely convoluted. Fig. 2(d) shows the results of the TGA analysis in air. The mass loss occurred at 575 ^{o}C, which is typical for well-graphitized carbon [34]. No mass loss attributed to amorphous carbon (<500 ^{o}C) was detected, evidencing that the CNFs produced were of high purity. In order to verify the stability of the CNF cathode, SEM images were taken before and after the NADH regeneration (Figs. 2(a, e) and Figs. 2(b, f), respectively). The results demonstrate that the CNF cathode was stable: there were no significant structural, morphological, and topographical changes.

3.2. Electrochemical NADH regeneration

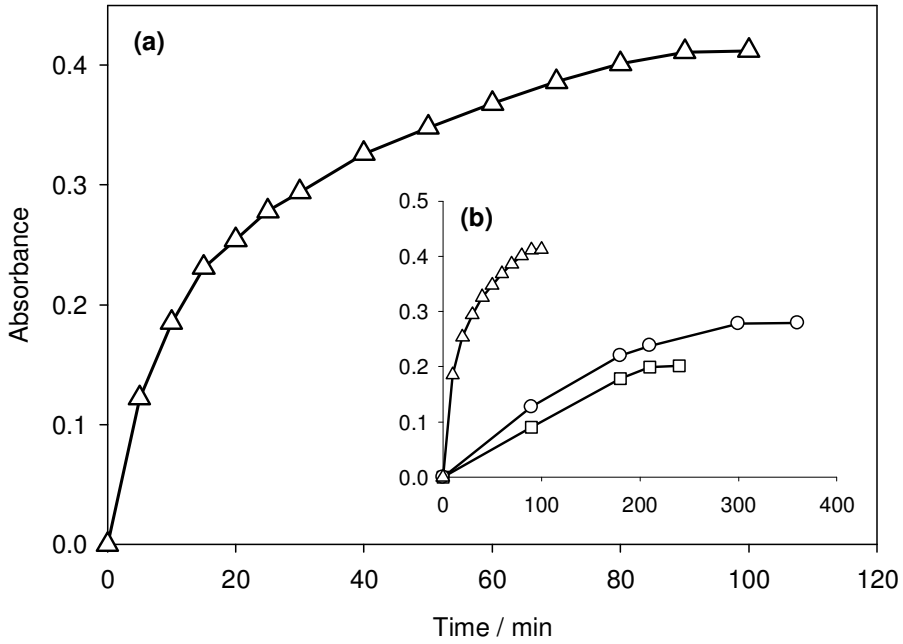

Figure 3. (*a*). Time dependence of absorbance at 340 nm recorded during the electrolysis of 1 mM NAD^+ in phosphate buffer in a batch electrochemical reactor operated at -2.3 V, using a CNF cathode. (*b*) Comparison of the CNF cathode response (triangles) to the response of the bare (CNF-free) stainless steel 316 mesh (circles) and a glassy carbon electrode (squares). The axis titles are the same as in (*a*). The geometric surface area of each electrode was 12.5 cm^2.

In order to investigate the NAD^+ reduction kinetics, and the efficiency of CNFs in producing (regenerating) enzymatically active 1,4-NADH from NAD^+, potentiostatic (electrolysis) experiments were performed in the batch electrochemical reactor at a fixed electrode potential of -2.3 V. The rationale for performing the regeneration at this potential is that our previous measurements on the 1,4-NADH regeneration in a batch electrochemical reactor employing a two-dimensional glassy carbon

electrode showed a 100% recovery of 1,4-NADH from NAD^+ without any production of non-enzymatically active NAD_2 and NADH isomers [31].

Fig. 3(a) shows the time evolution of absorbance at 340 nm, during the reduction of NAD^+ on the CNF cathode. The absorbance at 340 nm is related to the response of NADH isomers (including enzymatically-active 1,4-NADH) and the inactive dimer, NAD_2. Therefore, this result can only be used to monitor the progress of NAD^+ reduction reaction, but not the progress of 1,4-NADH formation [17, 18, 30, 31]. The result shows that after ca. 90 min, a plateau was reached indicating that reaction (semi)equilibrium had been reached. Using a UV/Vis absorbance vs. 1,4-NADH concentration calibration plot (not shown), and taking that only 1,4-NADH was produced by electrolysis (further in the paper it will be shown that this is the case), it has been determined that the NAD^+ conversion reached 48% after 90 minutes.

As we hypothesized, a cathode made of CNFs should offer a significant increase in the rate of NAD^+ reduction kinetics. Fig. 3(b) shows a comparison between the kinetics of NAD^+ reduction on the CNFs cathode to that on the glassy carbon cathode and a 316 stainless steel mesh cathode (note that all three electrodes geometric area exposed to the electrolyte was 12.5 cm^2). The result in Fig. 3(b) proves that our hypothesis is correct. Indeed, the kinetics of NAD^+ reduction is fastest on the CNF cathode. A NAD^+ reduction reaction (semi)equilibrium state on the CNF cathode was established after only 90 min, whereas it took 210 min on the glassy carbon electrode and 360 min on the stainless steel mesh to achieve (semi)equilibrium. In addition, the conversion of NAD^+ was also highest on the CNF cathode (48%), while the glassy carbon and stainless steel mesh cathodes yielded significantly lower levels (23 and 32%, respectively).

The next step in the attempt to prove the hypothesis was to determine the enzymatic activity of the product of NAD^+ reduction. Since the absorbance at 340 nm represents the response of various NADH isomers and of the inactive NAD_2 dimer, the actual percentage of 1,4-NADH (which is the only enzymatically-active product) present in the product mixture was determined by the enzymatic assay specified in the experimental section [15, 33]. The assay is based on the enzymatic conversion of substrate DL-lipoamide to product dihydrolipoamide using enzyme lipoamide dehydrogenase and 1,4-NADH as a co-factor [33]. This reaction requires a stoichiometric quantity of 1,4-NADH:

$$1,4-\mathrm{NADH} + \mathrm{DL\text{-}lipoamide} \xrightarrow{\text{lipoamide dehydrogenase}} \mathrm{NAD^+} + \mathrm{dihydrolipoamide} \qquad (1)$$

Therefore, a decrease in absorbance at 340 nm during the occurrence of reaction (1) due to the oxidation of 1,4-NADH to NAD^+ should be expected. Hence, the relative ratio of absorbance at 340 measured before reaction (1) starts, and after its completion, gives the percentage of enzymatically-active 1,4-NADH produced in the electrochemical reactor, using the CNF cathode. The assay was first calibrated using commercially available NADH that contains 98% of enzymatically-active 1,4-NADH.

The above enzymatic assay performed on samples taken from the reactor that employed the CNF cathode confirmed that 99.3 ± 0.6 % of the reduced NAD^+ was converted into enzymatically active 1,4-NADH, while the amount converted in the reactor that employed the stainless steel mesh was only 12 %. This proves that CNFs deposited on a stainless steel mesh are highly electrocatalytically active and selective towards conversion of NAD^+ into enzymatically active 1,4-

NADH. The fundamental origin of the increased electrocatalytic activity and selectivity of CNFs is the same as that on a glassy carbon electrode (discussed in our previous work [31]).

The electrochemical 1,4-NADH regeneration reaction is a heterogeneous reaction, occurring at the electrode surface. Hence, it was interesting to determine if the proceeds *via* NAD^+/NADH physisorption or chemisorption. Therefore, after the 1,4-NADH regeneration experiment was completed (Fig. 3), the infrared analysis of the CNF cathode surface was performed using the attenuated total reflectance (ATR) method.

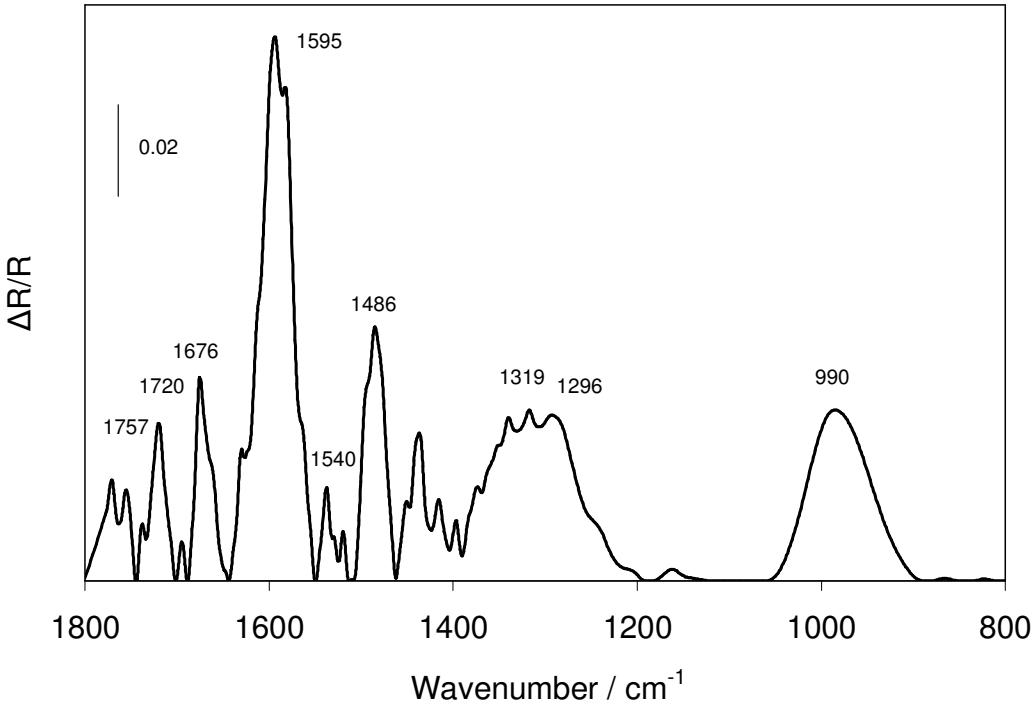

Figure 4. ATR spectrum of NAD^+ or 1,4-NADH adsorbed on a CNFs surface, recorded after the 1,4-NADH regeneration experiment (Fig. 3a) and subsequent thorough rinsing with deionized water.

The electrode was first thoroughly rinsed with deionized water. Thus, if either the reactant (NAD^+) or product (1,4-NADH) participated in the 1,4-NADH regeneration reaction through physisorption, no infrared peaks would be recorded by ATR. In the case of chemisorption, the molecule(s) would be attached to the CNFs surface by chemical bonds, and would not be desorbed by water rinsing. Fig. 4 shows the resulting ATR spectrum of the CNF sample after electrolysis at -2.3 V and rinsing. The spectrum shows characteristic peaks of NAD^+. The peaks at 1757 cm^{-1} and 1676 cm^{-1} are related to the response of the C=O stretch (nicotinamide) [35]. The vibration at 1630 cm^{-1} corresponds to the bending of NH_2 in the adenine moiety [35]. The broad peak at 1595 cm^{-1} and the minor peak at 1486 cm^{-1} represent the C_6-C_5 stretch (adenine) [35, 36] while the minor peak at 1540 cm^{-1} is the response of the C-N stretch [35]. Furthermore, the peak at 990 cm^{-1} is the representation of

ring stretch pyridine [37]. Hence, it is clear that the electrochemical 1,4-NADH regeneration reaction, preformed under the conditions employed in this paper, involves chemisorption of NAD^+ or/and 1,4-NADH, as one of the reaction steps.

4. CONCLUSIONS

The results presented here prove our hypothesis that a cathode made of CNFs grown on a stainless steel mesh enables fast electrochemical NAD^+ reduction kinetics. The cathode is also highly selective in reducing NAD^+ to enzymatically-active 1,4-NADH, yielding a 99.3 ± 0.6 % pure product. As such, the CNF cathode could be a good electrode candidate for regeneration of 1,4-NADH in biochemical reactors and biosensors. Based on our previous results with Pt- and Ni-patterned glassy carbon electrodes, a significant reduction in the 1,4-NADH regeneration potential (down to -1.6 V and -1.5 V, respectively) might be possible if the CNF cathode is also patterned with either Pt or Ni nano-particles. This, together with the high surface area of CNFs, would make the electrode more economically justifiable for its actual industrial use.

ACKNOWLEDGEMENTS
The authors would like to acknowledge the Natural Science and Engineering Research Council of Canada (NSERC), the Fonds de recherche du Québec - Nature et technologies (FRQ_NT), and the University of Engineering and Technology, Peshawar, Pakistan for providing the support for this research.

References

1. Y.H. Kim, Y.J. Yoo, *Enzyme. Microb. Technol*., 44 (2009) 129.
2. A. Liese, K. Seelbach, C. Wandrey, *Industrial Biotransformations*, Wiley-VCH, Weinheim (2006).
3. A.A. Karyakin, Y.N. Ivanova, E.E. Karyakina, *Electrochem. Commun*., 5 (2003) 677.
4. A. Schmid, J.S. Dordick, B. Hauer, A. Kiener, M. Wubbolts, B. Witholt, *Nature*, 409 (2001) 258.
5. Z.H. Huang, M. Liu, B.G. Wang, Y.P. Zhang, Z.A. Cao, G. G. Xuebao, CJPE, 6 (2006) 1011.
6. A.A. Sauve, *J. Pharmacol. Exp. Ther*., 324 (2008) 883.
7. N. Pollak, C. Dolle, M. Ziegler, *Biochem. J*., 402 (2007) 205.
8. A.C. Pereira, M.R. Aguiar, A. Kisner, D.V. Macedo, L.T. Kubota, *Sens. Actuators*, B, 124 (2007) 269.
9. P. Belenky, K.L. Bogan, C. Brenner, *Trends Biochem. Sci*., 32 (2007) 12.
10. K. Delecouls-Servat, A. Bergel, R. Basseguy, *Bioprocess Biosyst. Eng*., 26 (2004) 205.
11. A. Rongvaux, F. Andris, F. Van Gool, O. Leo, *BioEssays*, 25 (2003) 683.
12. R.A. van Santen, P.W.N.M. van Leeuwen, J.A. Moulijn, B.A. Averill, *Catalysis: An Integrated Approach*, Elsevier, Amsterdam (1999).
13. R. Devaux-Basseguy, A. Bergel, M. Comtat, *Enzyme. Microb. Technol*., 20 (1997) 248.
14. F. Pariente, F. Tobalina, M. Darder, E. Lorenzo, H.D. Abruna, *Anal. Chem*., 68 (1996) 3135.
15. A. Damian, K. Maloo, S. Omanovic, *Chem. Biochem. Eng*. Q., 21 (2007) 21.
16. A. Damian, S. Omanovic, *J. Mol. Catal. A: Chem*., 253 (2006) 222.
17. F. Man, S. Omanovic, *J. Electroanal. Chem*., 568 (2004) 301.

18. A. Azem, F. Man, S. Omanovic, *J. Mol. Catal. A: Chem*., 219 (2004) 283.
19. J. Moiroux, S. Deycard, T. Malinski, *J. Electroanal. Chem*., 194 (1985) 99.
20. P.J. Elving, W.T. Bresnahan, J. Moiroux, Z. Samec, *Bioelectrochem. Bioenerg*., 9 (1982) 365.
21. K. Takamura, A. Mori, F. Kusu, *Bioelectrochem. Bioenerg*., 8 (1981) 229.
22. H. Jaegfeldt, *Bioelectrochem. Bioenerg*., 8 (1981) 355.
23. C.O. Schmakel, K.S.V. Santhanam, P.J. Elving, *J. Am. Chem. Soc*., 97 (1975) 5083.
24. M. Beley, J.-P. Collin, *J. Mol. Catal*., 79 (1993) 133.
25. Y. Nakamura, S.I. Suye, J.I. Kira, H. Tera, I. Tabata, M. Senda, *Biochimica et Biophysica Acta - General Subjects,* 1289 (1996) 221.
26. E. Bojarska, B. Czochralska, *Bioelectrochem. Bioenerg*., 16 (1986) 287.
27. C.O. Schmakel, M.A. Jensen, P.J. Elving, *Bioelectrochem. Bioenerg*., 5 (1978) 625.
28. M. Aizawa, R.W. Coughlin, M. Charles, *Biotechnol. Bioeng*., 18 (1976) 209.
29. J.N. Burnett, A.L. Underwood, *Biochemistry*, 4 (1965) 2060.
30. I. Ali, A. Gill, S. Omanovic, *Chem. Eng. J*., 188 (2012) 173.
31. I. Ali, B. Soomro, S. Omanovic, *Electrochem. Commun*., 13 (2011) 562.
32. C.E. Baddour, F. Fadlallah, D. Nasuhoglu, R. Mitra, L. Vandsburger, J.L. Meunier, *Carbon*, 47 (2009) 313.
33. V. Massey, Q.H. Gibson, C. Veeger, *Biochem. J.,* 77 (1960) 341.
34. S. Yasuda, T. Hiraoka, D.N. Futaba, T. Yamada, M. Yumura, K. Hata, *Nano Lett*., 9 (2009) 769.
35. A. Damian, S. Omanovic, *Langmuir,* 23 (2007) 3162.
36. C. Nadolny, G. Zundel, *J. Mol. Struct*., 385 (1996) 81.
37. S. Bayari, A. Atac, S. Yurdakul, *J. Mol. Struct*., 655 (2003) 163